Supporting Information. Alexander T. Strauss, Lauren G. Shoemaker, Eric W. Seabloom, and Elizabeth T Borer. 2019. Cross-scale dynamics in community and disease ecology: relative timescales shape the community ecology of pathogens. *Ecology*.

APPENDIX S1

In this appendix, we present additional analyses and results that complement the main text. First, we illustrate the processes of dynamic superinfection (Fig. S1). Then, we show behavior of the superior competitor alone across gradients of its virulence (Fig. S2; single-species analog of Fig. 2) and the transmission coefficient (Fig. S3; single-species analog of Fig. 3). Next, we show behavior of the inferior competitor along across both gradients, both with and without the superior competitor (Fig. S4). Finally, we present a sensitivity analysis (Fig. S5).

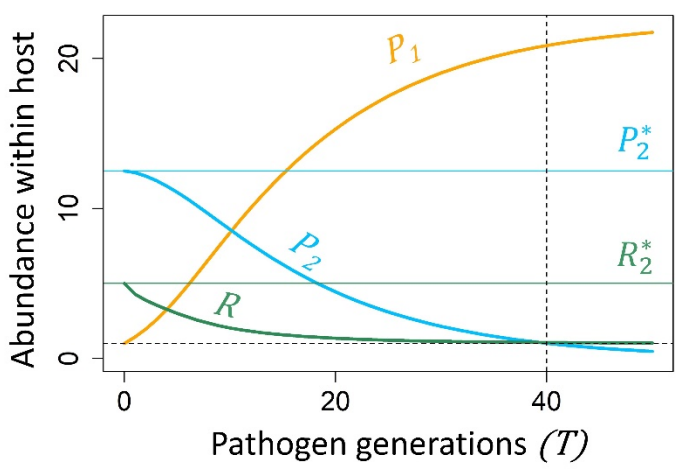

Fig. S1. *Dynamic superinfection.* Here we illustrate the process of dynamic superinfection (i.e., gradual competitive exclusion) when a host infected by the inferior competitor is invaded by the superior competitor. At the far left of this time series, the inferior competitor has reached its maximum within-host abundance (P_2^*) and depleted resources to its minimal resource requirement (R_2^*). If the superior competitor (orange; P_1) invades this host, resources immediately drop further (below R_2^*) and the inferior competitor begins to decline in abundance. However, the inferior competitor is not instantaneously eliminated. Instead, it transiently maintains an abundance above one (horizontal dashed line) for several pathogen generations (40 generations here). With relatively few pathogen generations per generation of hosts, (e.g., $T = 10$ or $T = 1$), the inferior competitor could be transmitted during this lag between invasion of the superior competitor and exclusion of the inferior competitor. Parameter values listed in Table 1 in the main text.

Superior competitor alone

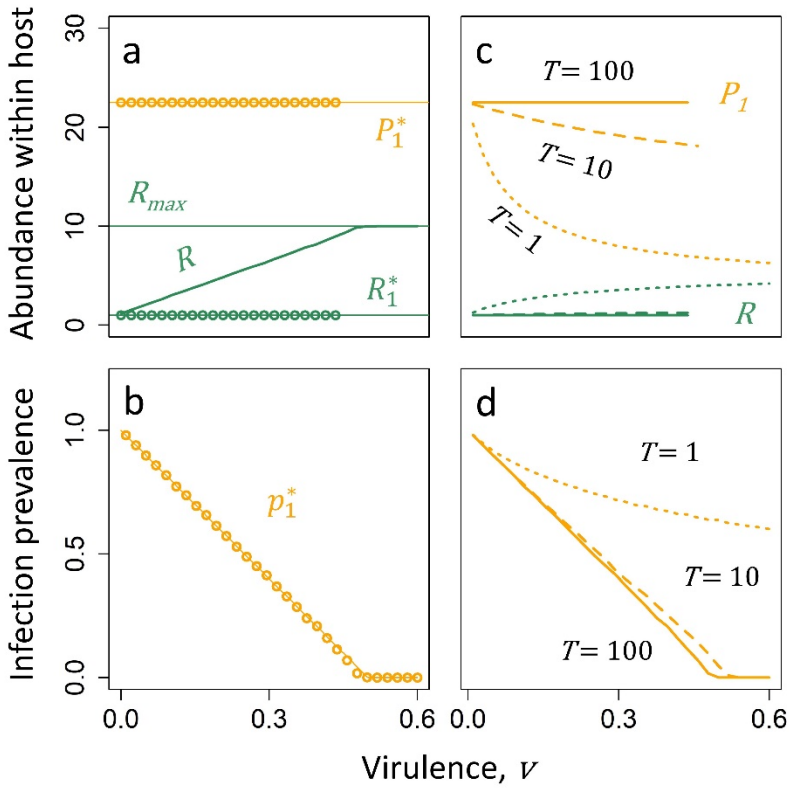

Figure S2. *Dynamics of the superior competitor alone across a gradient of its virulence.* The superior competitor behaves exactly as it does in the two-species case (Fig. 2 in the main text; all parameters identical here). **A-B)** Simulations of the hierarchical model (points) match analytical models (lines) when pathogens undergo many generations ($T = 100$) between each generation of hosts. **A)** Within infected hosts, pathogens approach P_1^* (orange) and resources approach R_1^* (green). Mean resources across the entire host population (R) increase as infection prevalence decreases. **B)** Infection prevalence approaches p_1^*: it decreases with virulence and excludes the pathogen at $v = 0.5$. **C-D)** Contours decrease the number of pathogen generations per generation of hosts (solid: $T = 100$; dashed: $T = 10$; dotted: $T = 1$). **C)** Slower dynamics (dashed: $T = 10$; dotted: $T = 1$) decrease the abundance of pathogens (orange) and increase the abundance of resources (green) within hosts. However, these effects disappear as virulence approaches zero. **D)** Slower dynamics also elevate infection prevalence due to exploitation-virulence, but not when virulence is very low.

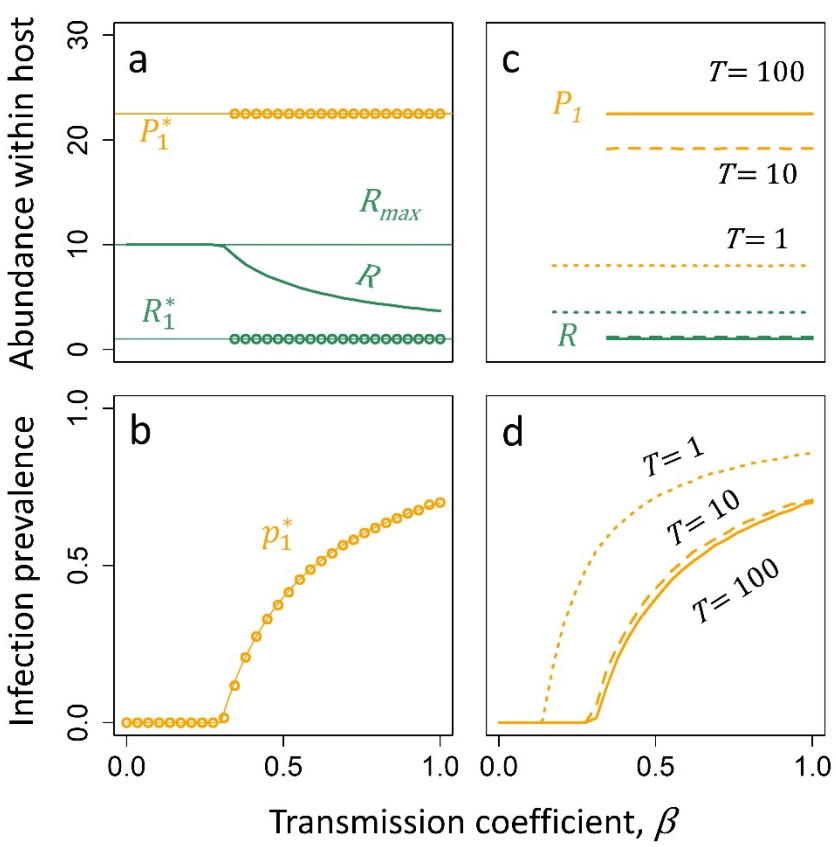

Figure S3. *Dynamics of the superior competitor alone across a gradient of the transmission coefficient.* The superior competitor behaves exactly as it does in the two-species case (Fig. 3 in the main text; all parameters identical here). **A-B)** Simulations of the hierarchical model (points) match analytical models (lines) when pathogens undergo many generations ($T = 100$) between each generation of hosts. **A)** Within infected hosts, pathogens approach P_1^* (orange) and resources approach R_1^* (green). Mean resources across the entire host population (R) increase as infection prevalence decreases. **B)** Infection prevalence approaches p_1^*: the pathogen invades at $\beta = 0.3$ and increases in prevalence with higher transmission. **C-D)** Contours decrease the number of pathogen generations per generation of hosts (solid: $T = 100$; dashed: $T = 10$; dotted: $T = 1$). **C)** Slower dynamics (dashed: $T = 10$; dotted: $T = 1$) depress the abundance of pathogens (orange lines) and increase the abundance of resources (green lines) within infected hosts. **D)** Slower dynamics also elevate infection prevalence due to exploitation-virulence.

Inferior competitor alone

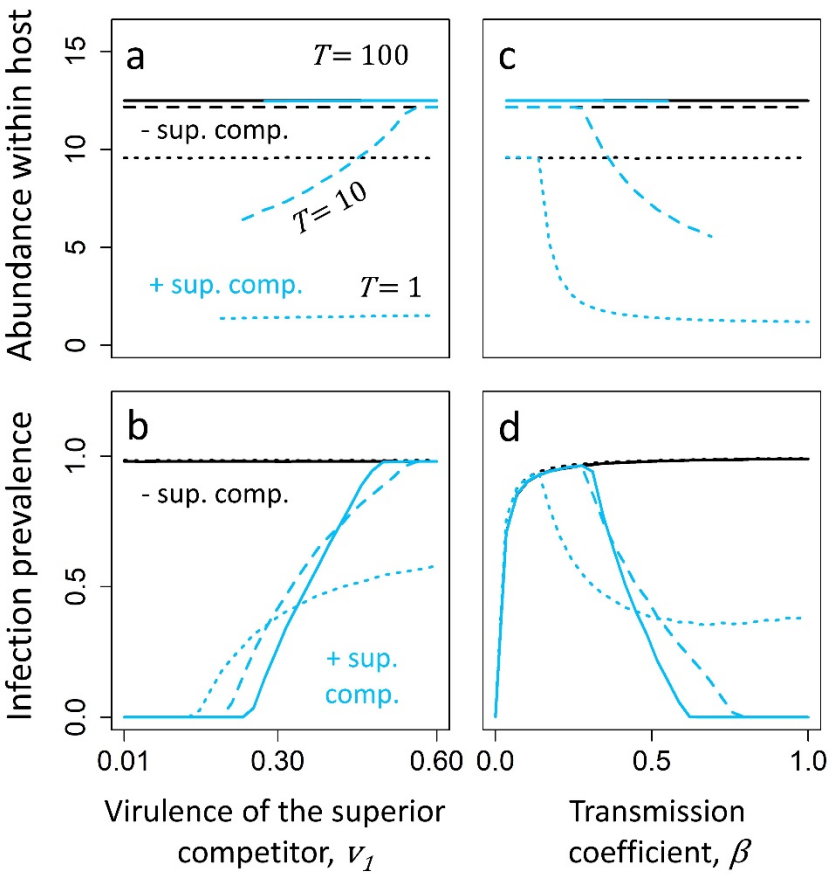

Figure S4. *The inferior competitor with and without the superior competitor: Partitioning impacts of exploitation-virulence from dynamic superinfection.* Lines plot the abundance (top row) and prevalence (bottom row) of the inferior competitor, in the absence (black) and presence (blue) of the superior competitor. Contours decrease the number of pathogen generations per generation of hosts (solid: $T = 100$; dashed: $T = 10$; dotted: $T = 1$). Columns recreate gradients of virulence of the superior competitor (left) and the transmission coefficient (right) from Figs. 2 and 3 in the main text, respectively (all parameters identical). In all cases, the difference in gray contours highlights the impacts of exploitation-virulence: With fewer pathogen generations per generation of hosts, pathogens do not deplete resources as low and do not induce such high virulence. Differences between gray and blue lines indicate the added impacts of dynamic superinfection.

Sensitivity analysis

We conducted a sensitivity analysis to investigate how variation in parameters that we did not vary in the main analyses affected behavior of our model. We constrained the three parameters that we did vary in the main analyses: virulence of the superior competitor ($v_1 = 0.3$), the transmission coefficient ($\beta = 0.5$), and relative pathogen generation time ($T = 1$). We varied all of the other parameters: resource supply rate (s), maximum resources (R_{max}), reproductive rate of the superior competitor (u_1), reproductive rate of the inferior competitor (u_2), death rate of both pathogens (m), the resource quota of both pathogens (q), background death rate of uninfected hosts (d), and virulence of the inferior competitor (v_2). We ran 10,000 simulations of the hierarchical model with each of these parameters drawn from uniform distributions. The parameters from the competition model within hosts (s, R_{max}, u_1, u_2, m, and q) ranged from 20% under to 20% over values used in the main analyses (see Table 1 in the main text). The parameters for host death (d and v_1) ranged from 0.00 to 0.05. Each parameter was standardized by subtracting its mean and dividing by its standard deviation. We then used multiple regression to obtain standardized effect sizes for the influence of each parameter on each response variable. Response variables included infection prevalence of each pathogen, the prevalence of coinfections, and the mean abundance of each pathogen within hosts.

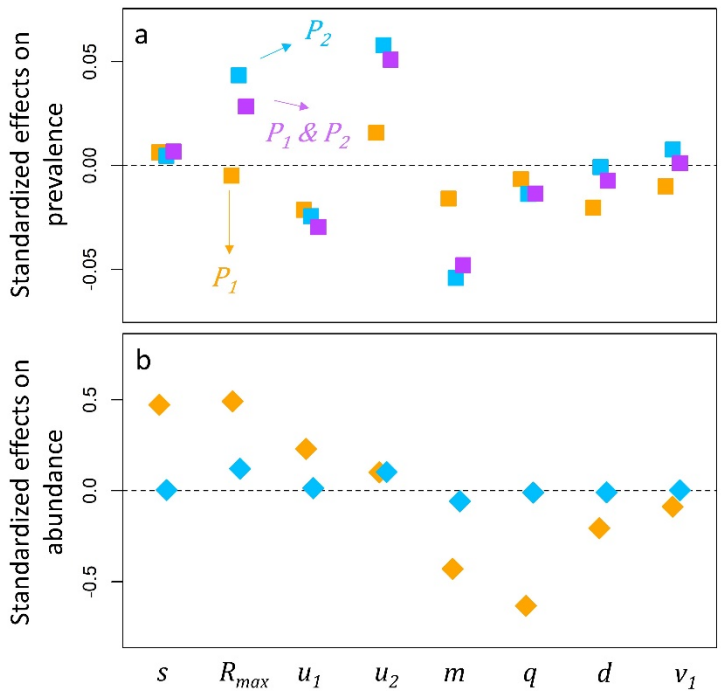

Figure S5. *Sensitivity analysis when host and pathogen generation times are equal (T = 1).* Standardized effect sizes show the impact of each parameter on infection prevalences (top) and the abundance of pathogens within hosts (bottom). **A) Infection prevalence:** In general, prevalence of the inferior competitor (blue) and prevalence of coinfections (purple) are more sensitive than prevalence of the superior competitor (orange). Prevalence of the inferior competitor and coinfections are especially sensitive to the maximum abundance of resources (higher R_{max} increases both), reproductive rate of the inferior competitor (higher u_2 increases both), and death rate of both pathogens (higher m decreases both). **B) Abundance of pathogens within hosts:** In general, abundance of the superior competitor (orange) is more sensitive than abundance of the inferior competitor (blue). Abundance of the superior competitor is especially sensitive to the supply rate of resources (higher s increases it), maximum resource abundance (higher R_{max} increases it), pathogen death rate (higher m decreases it) and the resource quota of pathogens (higher q decreases it).